

Emergent organization of oscillator clusters in coupled self-regulatory chaotic maps

HIROYASU ANDO^{1,3,*}, SUDESHNA SINHA² and KAZUYUKI AIHARA^{1,3}

¹Aihara Complexity Modelling Project, ERATO, JST, 4-1-8, Honcho, Kawaguchi, Saitama, Japan

²The Institute of Mathematical Sciences, CIT Campus, Taramani, Chennai 600 113, India

³Institute of Industrial Science, The University of Tokyo, 4-6-1 Komaba, Meguro-ku, Tokyo 153-8505, Japan

*Corresponding author. E-mail: andoh@sat.t.u-tokyo.ac.jp

Abstract. Here we introduce a model of parametrically coupled chaotic maps on a one-dimensional lattice. In this model, each element has its internal self-regulatory dynamics, whereby at fixed intervals of time the nonlinearity parameter at each site is adjusted by feedback from its past evolution. Additionally, the maps are coupled sequentially and unidirectionally, to their nearest neighbor, through the difference of their parametric variations. Interestingly we find that this model asymptotically yields clusters of superstable oscillators with different periods. We observe that the sizes of these oscillator clusters have a power-law distribution. Moreover, we find that the transient dynamics gives rise to a $1/f$ power spectrum. All these characteristics indicate self-organization and emergent scaling behavior in this system. We also interpret the power-law characteristics of the proposed system from an ecological point of view.

Keywords. Self-organization; power-law scaling; chaos control; $1/f$ noise; coupled map lattices.

PACS Nos 05.45.Gg; 05.45.Ra; 05.65.+b

1. Introduction

Spatially extended systems composed of many interacting nonlinear elements are capable of displaying rich dynamical behavior and thus have gathered attention in the field of nonlinear dynamics. Foremost among such models are those of coupled maps on a lattice. This class of models has provided test-beds for investigating spatiotemporal patterns in a variety of contexts in physics, biology and engineering [1].

Here we introduce a model of parametrically coupled logistic maps on a one-dimensional lattice. In this model, each element has its internal self-regulatory dynamics, whereby at fixed intervals of time the nonlinearity parameter at each site is adjusted by feedback from its past evolution. Additionally, the maps are coupled sequentially, unidirectionally, to their nearest neighbor, through the difference of

their parametric variations. The coupling propagates only if the variation at a site exceeds the coupling amount received from the preceding site. This cascade of coupling is reminiscent of avalanches of activity in models with threshold activated coupling, such as sandpile-like models, with the nonlinearity parameter of each map being analogous to height. The specifics of the model are discussed in §2.

2. Model

Let us consider the following system with the two-dimensional map:

$$x_{n+1} = f(x_n, a_n), \quad n = 0, 1, \dots, \tilde{T}, \quad (1)$$

$$a_{n+1} = g(n, x_n, a_n), \quad (2)$$

where x_n is the state variable at time n and a_n is the dynamically changing nonlinearity parameter. The function $f(\cdot, \cdot)$ can be taken to be a one-dimensional unimodal function, with varying nonlinearity a_n . Note that a_n determines the height of the unimodal map. In this work, we consider the logistic form for f , namely $f(x_n, a_n) = x_{n+1} = a_n x_n (1 - x_n)$ with $0 \leq a_n \leq 4$ and $0 \leq x_n \leq 1$.

The function g is the feedback adjustment function introduced in ref. [2], and it depends on n , x_n and a_n . It is described explicitly as follows:

$$g(n, x_n, a_n) = \begin{cases} 4\hat{x}_j & \text{if } n = jT, \\ a_n & \text{if } n \neq jT, \end{cases} \quad j = 1, 2, 3, \dots, \quad (3)$$

$$\hat{x}_j = \max\{x_l\}_{(j-1)T < l \leq jT}, \quad (4)$$

where T is an integer parameter.

These equations describe how the nonlinearity a_n changes its value every T steps, influenced by the largest value of x in the preceding T steps, $(j-1)T < n \leq jT$. Now the maximum x , \hat{x} , of the logistic map function $f(x) = ax(1-x)$ is $a/4$, i.e. the nonlinearity a is $4\hat{x}$. So eq. (3) implies that the nonlinearity adapts to the ‘effective nonlinearity’ of the (finite time) dynamics of the preceding T steps given by $4\hat{x}$. This adaptation of the nonlinearity a will stop when its dynamics reaches a fixed point, i.e., $a_{n+1} = a_n = a^*$, and this will happen only when the T steps include the maximum point of the logistic function with nonlinearity a^* . Since a point passing through the maximum has slope zero, it is a point on a superstable cycle. So this mechanism internally adapts the nonlinearity to a value yielding some superstable periodic orbit. Note that the value of $a_j(i)$ by the update rules (3) and (4) is always decreasing, because the logistic map is upward humped [2].

Now T gives the length of the time series that determines the change in the value of the nonlinearity. It also gives the time scale at which the parameter a_n updates, namely it sets a time scale for variation of a which is T times slower than the updating of the state variable. So x can be considered the fast variable and a the slow variable in this dynamical system.

As mentioned before, after successive iterations of the maps (1)–(4), a_j converges to a value so that the orbit of x_n is superstable periodic. Such superstable periodic orbits mainly exist in the periodic windows observed in the bifurcation diagram of the logistic map. The mechanism of the convergence is elucidated in detail in ref. [2].

Emergent organization of oscillator clusters

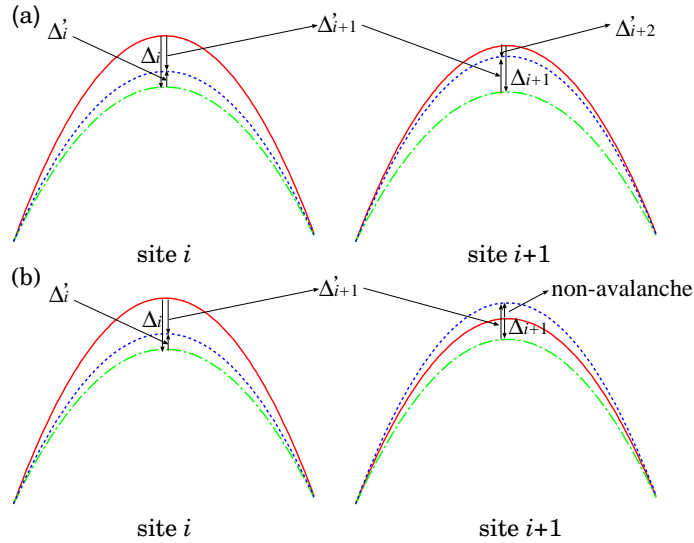


Figure 1. The schematic figure illustrating the nature of the avalanche-like coupling. (a) There is avalanche from site $i + 1$ to site $i + 2$. (b) No avalanche occurs from site $i + 1$ to site $i + 2$.

Now we investigate a spatially extended system of size N , composed of logistic maps with nonlinearities adjusted by the above feedback mechanism. In our model, at discrete time n , the state variable of the element at site i and its nonlinearity parameter is denoted by $x_n(i)$ and $a_n(i) (\equiv a_j(i), j = [n/T])$. The site index $i = 1, \dots, N$, where N is the number of sites in the system.

First, each element is updated by the map (1) for T time steps. Let us call such updates *internal dynamics*. Then there is a change in the nonlinearity of the elements by feedback from the preceding T steps by eq. (4). After this internal self-regulatory parametric adjustment, there is a coupling among the elements. In analogy with sandpile-like models, the ‘height’ of each element is given by $a_j(i)$, which determines the maximum of local unimodal function determining the internal dynamics. Then, the change in the height $a_j(i)$ of each element i by eq. (4) is denoted by Δ_i , where $\Delta_i = a_{j-1}(i) - a_j(i)$ and $\Delta_i \geq 0$. This change in height Δ_i is the quantity that influences the neighboring site, and determines the form of the coupling (see figure 1).

Now we couple the elements in a manner reminiscent of *avalanche coupling* [3,4], with the coupling being unidirectional and sequential, occurring from site 1 to N . In our scheme, for elements $i = 2, \dots, N$, if the height drop of an element is larger than the height drop of the preceding element then the difference in the height drops (i.e. parameter changes) is added to the next element.

Explicitly this gives the following condition for coupling to occur, i.e. for an avalanche to propagate. Let Δ_i' be defined recursively as follows: $\Delta_i' = \Delta_{i-1} - \Delta_{i-1}'$, $i = 2, \dots, N - 1$. If $\Delta_i' < \Delta_i$, then $\Delta_i - \Delta_i'$ is added to $a_j(i + 1)$, and zero otherwise. So coupling is propagated, that is an avalanche occurs, when

the parametric variation of a site is larger than that of the preceding element (see figure 1).

The boundary conditions are given as follows: $\Delta'_1 = 0$ and so $\Delta'_2 = \Delta_1$, i.e. the variation Δ_1 is always added to $a_j(2)$. At the other end, the boundary at element N is open.

After the sequential coupling finishes, each element is updated again by the *internal dynamics* given in eqs (3) and (4). Then, the coupling interactions, giving rise to the next avalanche, start. The number of the sites influenced by coupling during the avalanche process between chaotic updates indicates the *avalanche size*. Here we will study the *normalized avalanche size*, i.e., the avalanche size divided by system size N , denoted by $s(j)$. Note that this quantity is bounded between 0 and 1.

Relevance of the model to food chains: In general, an ecosystem is a web of complex interactions among species. To understand this complexity, it is necessary to study basic food chain dynamics. Food chains describe the feeding relationships between species in an ecological community. They graphically represent the transfer of material and energy from one species to another within an ecosystem. Organisms are connected to the organisms they consume, and this determines the direction of biomass transfer [5–7].

Food chains involving three or more species are then the fundamental building blocks for ecosystems. While a particular ecosystem may be intractable, simple food chains can be modeled by coupled nonlinear maps, as in this work. So our class of models may provide an illustrative paradigm within which food-chain models can be analyzed, thus shedding light on ecocomplexity in general.

Specifically, organisms in a food chain are usually grouped into trophic levels, where each trophic level may consist of either a single species or a group of species that are presumed to share both predators and prey. They usually start with a primary producer and end with a carnivore. In our model the nodes/sites) can represent trophic levels. The first site represents photosynthesizing plants and the open end represents the carnivores at the top of the food chain. The unidirectional coupling among nodes along the chain can then mimic the connections from one organism to the next in the food chain.

The dynamics at each site/node in our chain models the population dynamics at the trophic level through the logistic map [8]. The effective growth rate is given by the nonlinearity parameter at each node. Now each level has an internal feedback mechanism that drives the level to stable cyclic population patterns. This is given by eqs (1)–(4). Now, since the levels are connected, the effective growth rates at each level must depend on the level below it in the chain. This is reflected in our coupling scheme, which couples the effective growth rates of the population in adjacent connected levels.

In our coupling the rate of change of effective growth rates due to the internal feedback at one level influences the change at the next level in the chain. If this change is larger than the change at the lower level, it is reduced by an amount proportional to the difference of the changes of growth rates. This has the effect of smoothing out differences in growth rate changes, and is akin to threshold activated coupling in parameter space. Here we will investigate in detail the nature of the emergent population dynamics of this chain under this coupling.

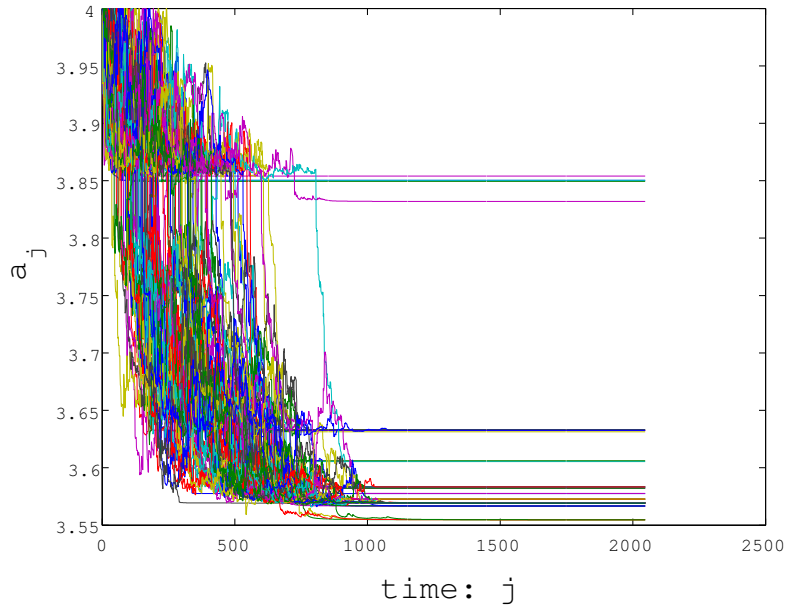


Figure 2. Superimposed time series of $a_j(i)$, for $T = 50$, $\tilde{T}/T = 2048$ and $N = 100$. It is evident that after complex transient dynamics (up to $j \sim 1000$), one obtains almost steady $a_j(i)$ values.

Further, note that from the theoretical point of view we are distinct from the more commonly studied class of models which couple state variables [1]. In contrast, we are coupling the fluctuations of nonlinearity parameters.

In the next section, we show the numerical results of the spatiotemporal behavior of this system and analyze them from the statistical point of view. Since the attractor of each individual element is a superstable periodic orbit, the avalanche-coupled maps are expected to relax to sets of superstable oscillatory states. However, the *interactive effects of the avalanches give rise to long-range correlations*, and the relaxation to periodic orbits is not trivial, unlike the case of a single self-regulatory element. In fact, our results show that the emergent state is composed of *clusters* of superstable periodic orbits, with *power scaling characteristics*.

3. Results

Figures 2 and 3 show the time evolution of the nonlinearity parameters of the elements, under self-regulatory internal dynamics and avalanche coupling. It is clearly evident that the system evolves to clusters of oscillators having different periodicities. That is, the asymptotic state displays sets (clusters) of contiguous elements, where each set is characterized by a parameter value determining the periodicity of the oscillators in that set. Indeed, figure 4 shows the periodic behavior in one of the clusters observed in figure 3. The phases of the periodic orbits in the cluster are not the same but the periods, i.e. period 32, are the same.

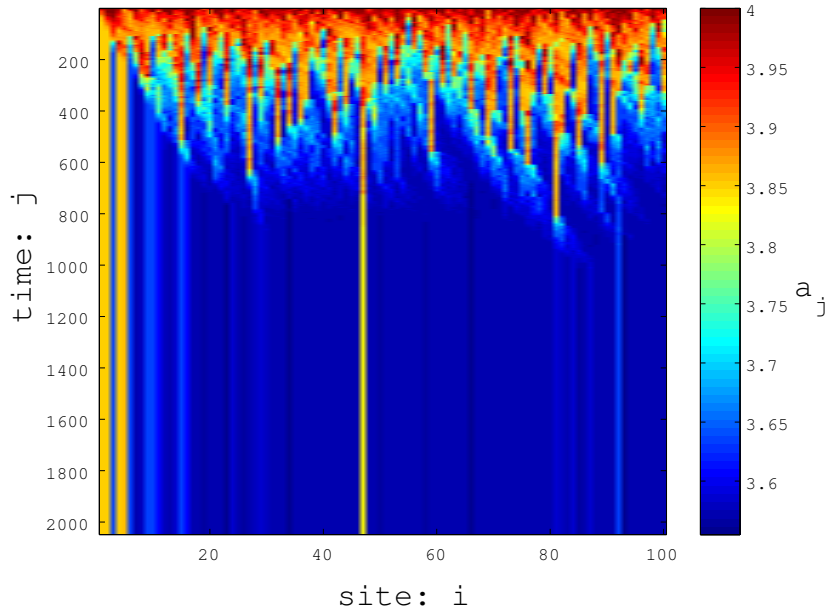


Figure 3. Spatiotemporal pattern of $a_j(i)$, starting from random initial $x(i)$ and initial $a(i) = 4$. The color shows the values of $a_j(i)$. $T = 50$, $\bar{T}/T = 2048$ and $N = 100$.

Figure 5 shows the time evolution of the averaged normalized avalanche size $s(j)$. Notice that the saturating behavior of $s(j)$ is counterintuitive, since avalanches still occur at almost all the sites after their relaxation. However, the amount of coupling arising from such avalanches, namely the Δ 's, are extremely small (see the inset in figure 5). These small widespread avalanches are due to convergence processes of each element by the internal feedback dynamics. That is, a_j is not converged completely, but very slowly evolving towards an asymptotic value. Since $a_j - a_{j+1}$ is very small, the dynamical changes in the system due to the avalanches is insignificant in the saturated regime. So the system evolves from large coupling exchanges involving few sites (with very significant dynamical consequences) to very small coupling transfers involving almost the entire system.

Figure 6 shows the power spectrum of avalanche size $s(j)$. The power spectrum is averaged over 100 runs of 1024 each, with respect to the time scale of j , and sampled around the transition of $s(j)$. Low frequency fluctuations are clearly evident from the spectra, as one finds

$$P(f) \sim 1/f^\alpha$$

at the low frequency end, with $\alpha \sim 1$.

We also investigate the effect of system size N and T on the time evolution of the avalanche size. Figure 7 shows the normalized $s(j)$ for six different sizes N and $T = 50$, averaged over 8 runs of 2048 each. We define *transience time* as the time required to reach the saturation value of $s(j)$. It is clear from figure 7 that the transition to the saturated value of $s(j)$ gets sharper with increasing system size. However, the transience time does not appear to be much influenced by N .

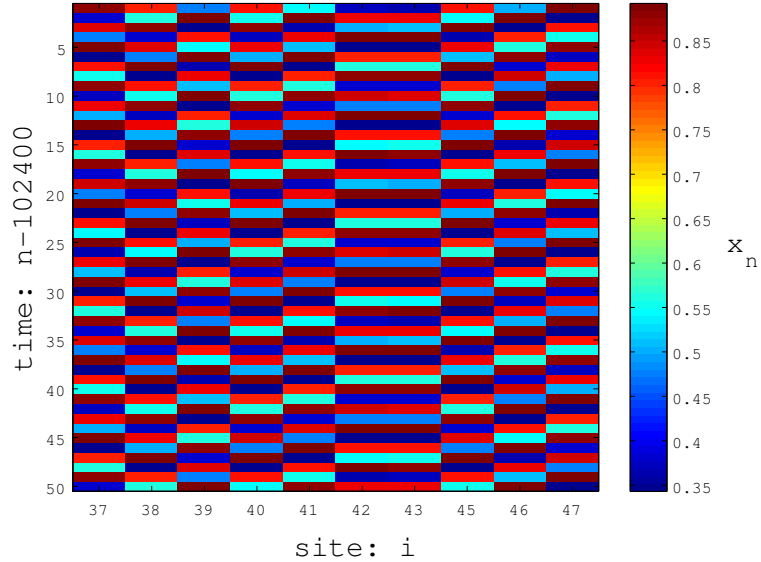


Figure 4. The last 50 steps of time series for $x_n(i)$ in one of the clusters observed in figure 3. The cluster is selected in the range $37 \leq i \leq 47$. The color shows the values of $x_n(i)$.

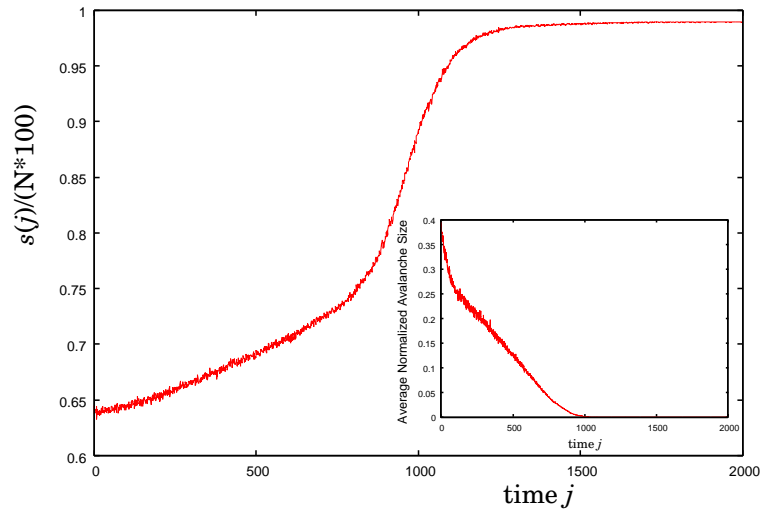


Figure 5. Time evolution of avalanche size $s(j)$ averaged over 100 runs. (Inset) The sum over coupling amounts in an avalanche (i.e. sum over Δ 's) as a function of time j averaged over 100 runs. $T = 50$, $\tilde{T}/T = 2000$ and $N = 100$.

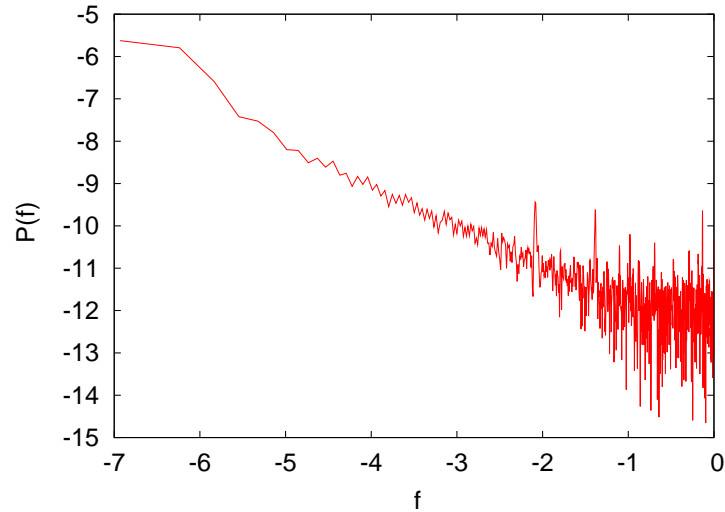


Figure 6. Power spectrum of avalanches, averaged over 100 runs, with $T = 50$, \tilde{T}/T from 1000 to 2024 and $N = 100$.

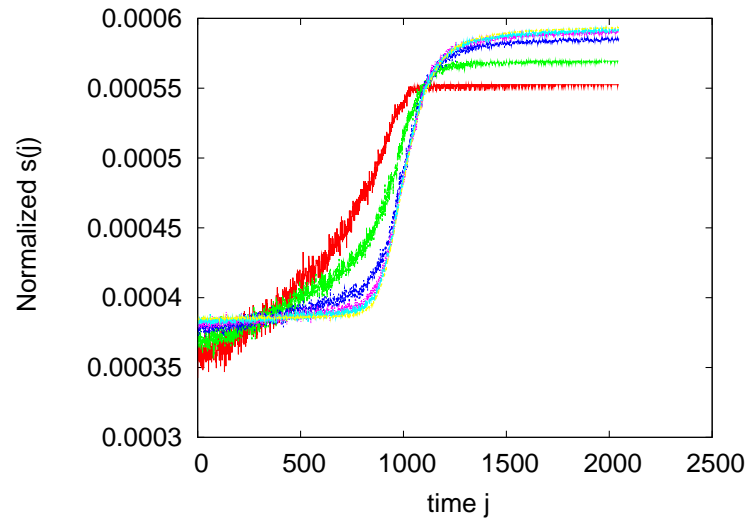


Figure 7. Time evolution of the normalized $s(j)$ averaged over 8 trials for several sizes N . Red, green, blue, magenta, aqua and yellow correspond to $N = 50, 100, 250, 500, 1000$ and 10000 , respectively. $T = 50$.

Figure 8 (top) represents the histograms of the number of converged elements with respect to time j , for several T values. For $T = 50$, we can find the peak of the converged elements at around the saturating time in figure 7, i.e. $j \simeq 1000$. Moreover, the histograms for different T values show exponential dependence of transience time on T . This is also clearly seen in figure 8 (bottom). Thus, we may

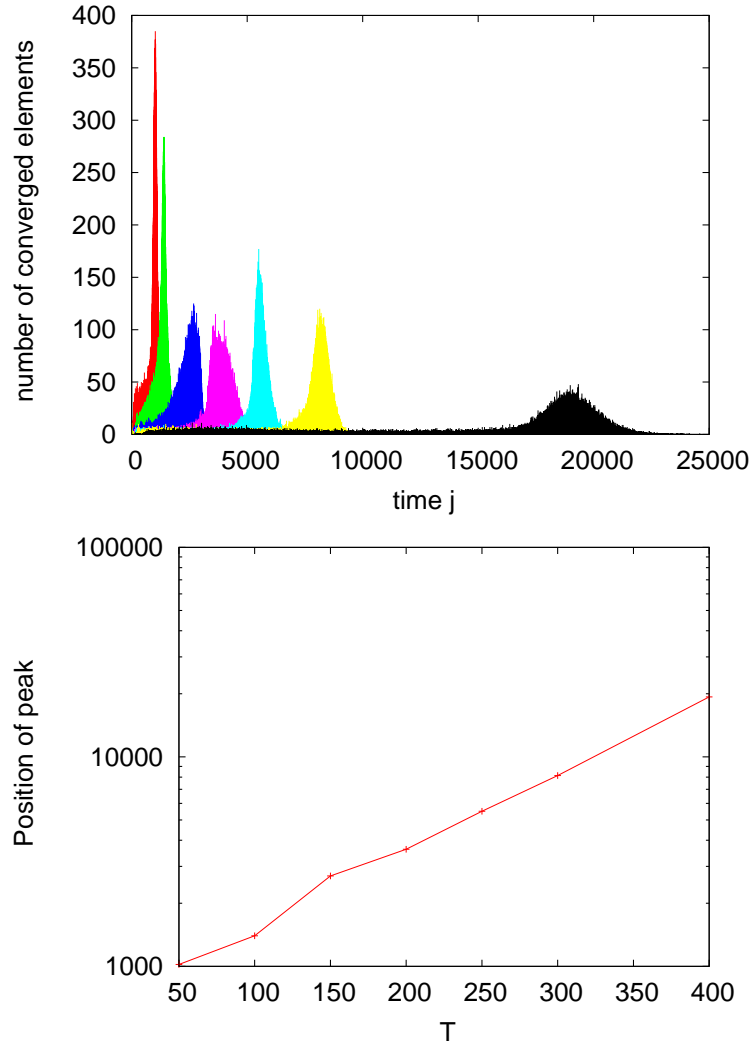


Figure 8. (Top) Histogram of converged elements at the time j for several T . Red, green, blue, magenta, light blue, yellow and black represent $T = 50, 100, 150, 200, 250, 300$ and 400 , respectively. (Bottom) The peak position in the histograms with respect to T . The vertical scale is logarithmic.

conclude that the transience time does not depend on the size N , when N is large enough. However, the transience time depends crucially on T , with the dependence being exponential.

As can be seen in figures 2 and 3, the relaxed states consist of oscillator clusters in the spatial domain. Figure 9 shows the probability of finding a cluster of size c with respect to c , with the cluster size c determined to an accuracy of ϵ . It is evident that the clusters have a *power-law distribution*, truncated by an exponentially falling

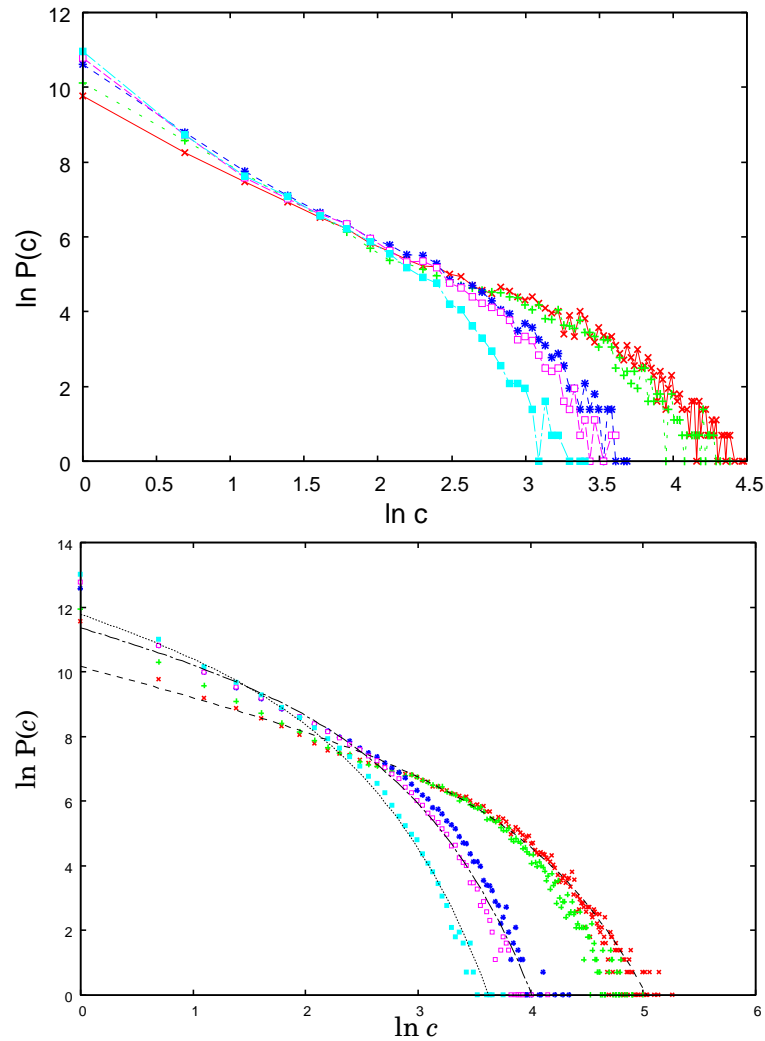


Figure 9. Distribution of the cluster size c with $T = 100$ and N equal to 100 (above) and 1000 (below), for several values of precision ϵ . The red, green, blue, magenta and light blue represent $\epsilon = 0.001, 0.0005, 0.0001, 0.00005$ and 0.00001 , respectively. The fitting function in the bottom panel is $P(c) \sim c^{\gamma_1} \exp(-c/\gamma_2)$. The dashed ($\gamma_1 = 0.9, \gamma_2 = 27$), dashed-dotted ($\gamma_1 = 0.9, \gamma_2 = 7$) and dotted ($\gamma_1 = 1.0, \gamma_2 = 4.5$) curves fit red, magenta and light blue points, respectively.

tail. In figure 9 (bottom), we also show the fitting function which can be described as $P(c) \sim c^{\gamma_1} \exp(-c/\gamma_2)$. This function represents a power-law with exponential cut-off in the higher degree.

It should be noticed that the slope of the region showing power-law scaling in figure 9 is almost 1. Moreover, we also find the $1/f$ fluctuation in the time evolution

of $s(j)$ in figure 6. These results imply that our model has analogy with the sandpile model proposed in ref. [9].

4. Discussion and conclusion

We have presented a simplified picture of interacting population dynamics with adaptive self-regulatory feedback. Nevertheless our abstract model provides a scenario where the adaptive populations can, under coupling, lead to organization into clusters characterized by power-law distributions.

4.1 Interpretation 1: Power-law scaling of trophic links

The general direction of the internal adaptive change is to ensure regular stable cyclic population dynamics. When a species undergoes a parametric change, it changes the adaptive process of the species in its neighbouring level. In the beginning the nonlinearities (growth rates) at each level, are unrelated to each other, but the coupling soon ensures that long-range correlations develop. So from random distributions, the system naturally organizes into clusters, whereby contiguous levels have population cycles of the same period. This correlation in population dynamics can be regarded as an effective link. Since c species are strongly correlated in the cluster of size $c - 1$, each of them can be considered to have c links.

Note that when we redraw the relation between the cluster with c links (i.e., the cluster of size $c - 1$) and the probability distribution of $P(c)$, it also has power law distribution (not shown here).

Recently, truncated power-law relation between the number of trophic links and their cumulative distribution have been observed in empirical food webs [10]. Thus the above interpretation, based on the ansatz that the oscillator clusters effectively have strong links among themselves, provides a reasonable scenario for the emergence of power-law scaling in the distributions of trophic links. Further, the power-law relations are truncated at high degrees, just as the power-law distributions arising in our model (as is evident in figure 9).

4.2 Interpretation 2: Power-law scaling in taxa-subtaxa distributions

From the viewpoint of biological diversity, the self-organized clusters may be interpreted as taxa with different number of subtaxa which have emerged as a result of co-evolutionary processes. Here, the size of subtaxa in a taxon is represented by the number of elements in the cluster. As mentioned above, the clusters are naturally organized from the initially random states, due to correlations arising from inter-species interactions. Therefore, the time evolution of our system can be interpreted as co-evolutionary adaptive processes.

As a matter of fact, an examination of size-frequency distributions of taxa with different numbers of subtaxa has shown power-law scaling characteristics in refs [11]. If the size of our clusters is considered as the number of subtaxa within the

taxon, the size–frequency distribution of taxa with subtaxa in our model also shows power-law in their size distributions in lower degree.

4.3 *General relevance*

Lastly, this model is of general interest as it involves the coupling of chaotic systems through variations in their parameters, rather than the usual diffusive coupling of their state variables. Here the interaction arises from the influence of the (slow) adaptive changes of the nonlinearity parameter of the individual systems, on each other. So as a theoretical construct it is quite distinct from the usual coupled map lattice models that have been extensively studied in literature [1]. From the viewpoint of model-building, the results of this case study are of considerable interest.

In summary, we have investigated parametrically coupled logistic maps with internal self-regulatory feedback mechanisms. We find an emergent state characterized by clusters of superstable orbits. These clusters display power-law scaling, suggesting an interesting organization of the interactive populations.

References

- [1] K Kaneko (ed), *Theory and applications of coupled map lattices* (Wiley, 1993) and references therein
- [2] H Ando and K Aihara, *Phys. Rev.* **E74**, 066205 (2006)
- [3] S Sinha and D Biswas, *Phys. Rev. Lett.* **71**, 2010 (1993)
- [4] S Sinha, *Phys. Rev.* **E49**, 4832 (1994); *Int. J. Mod. Phys.* **B9**, 875 (1995)
- [5] L Stone, *Nature (London)* **365**, 617 (1993)
- [6] E P Odum, *Fundamentals of ecology*, 2nd ed. (W B Saunders Co., Philadelphia, 1959)
- [7] G E Hutchinson, *An introduction to population ecology* (Yale, 1978)
- [8] R M May, *Nature (London)* **261**, 459 (1976)
- [9] P Bak, C Tang and K Wiesenfeld, *Phys. Rev.* **A38**, 364 (1988)
- [10] J M Montoya, S L Pimm and R V Solé, *Nature (London)* **442**, 259 (2006)
- [11] B Burlando, *J. Theor. Biol.* **146**, 99 (1990)
B Burlando, *J. Theor. Biol.* **163**, 161 (1993)